Spin susceptibility of underdoped cuprate superconductors: Insights from a stripe-ordered crystal

M. Hücker, G. D. Gu, and J. M. Tranquada
Brookhaven National Laboratory, Upton, New York 11973-5000, USA
(Received 6 November 2008; published 5 December 2008)

We report a detailed study of the temperature and magnetic-field dependence of the spin susceptibility for a single crystal of $La_{1.875}Ba_{0.125}CuO_4$. From a quantitative analysis, we find that the temperature-dependent anisotropy of the susceptibility, observed in both the paramagnetic and stripe-ordered phases, directly indicates that localized Cu moments dominate the magnetic response. A field-induced spin-flop transition provides further corroboration for the role of local moments. Contrary to previous analyses of data from polycrystalline samples, we find that a commonly assumed isotropic and temperature-independent contribution from free carriers, if present, must be quite small. Our conclusion is strengthened by extending the quantitative analysis to include crystals of $La_{2-x}Ba_xCuO_4$ with $x=0.095$ and 0.155. On the basis of our results, we present a revised interpretation of the temperature and doping dependence of the spin susceptibility in $La_{2-x}(Sr,Ba)_xCuO_4$.

DOI: 10.1103/PhysRevB.78.214507 PACS number(s): 74.72.Dn, 74.25.Ha

I. INTRODUCTION

A central controversy in the field of high-temperature superconductivity concerns the nature of the magnetic response in the normal state: does it come from local moments or mobile conduction electrons? The bulk spin susceptibility, χ^s, has been central to the discussion, but the analysis so far has been ambiguous. For example, in underdoped cuprates one experimentally observes a decrease in the normal-state χ^s on cooling below some characteristic temperature T_{max}.[1] When this behavior was first identified in underdoped $YBa_2Cu_3O_{6+x}$ through measurements of the Y Knight shift by Alloul *et al.*,[2] it was interpreted as evidence for the development of a pseudogap in the electronic density of states. Such a perspective attributes the bulk magnetic response to paramagnetism of the conduction electrons (Pauli paramagnetism), and it is often cited.[3–5] In contrast, Johnston[6] proposed that $\chi^s(T)$ consists of the following two components: (1) a temperature-dependent portion that scales with doping and that is associated with antiferromagnetically correlated Cu moments, and (2) a Pauli contribution that happens to be roughly proportional to the doped hole density. This alternative approach also remains popular.[7–9]

Clearly, the temperature dependence of χ^s is closely tied to the issue of the pseudogap,[10] a continuing conundrum and challenge. The nature of the spin response is also part of the ongoing discussion on the dynamic susceptibility, where the momentum- and energy-dependent structure observed by neutron scattering has generally been interpreted either as the response of conduction electrons scattering across the Fermi surface[11–13] or as fluctuations of local Cu moments.[14,15] While there is much debate on the dynamic response, we have seen little critical discussion of the alternative interpretations of the static susceptibility, or reconsideration of the assumptions that went into analyses first developed two decades ago, typically applied to measurements on polycrystalline samples.[6,7]

In this paper, we present bulk susceptibility measurements performed on a single crystal of $La_{1.875}Ba_{0.125}CuO_4$. We go through a stepwise analysis of the data, considering the extent to which we can distinguish between contributions from mobile charge carriers and local moments. One criterion for such a distinction is anisotropy: Pauli paramagnetism is expected to be isotropic, whereas the paramagnetic response of local moments depends on the orientation of the applied field due to anisotropic gyromagnetic factors. Thus, from the fact that we observe a temperature-dependent anisotropy of the susceptibility in the paramagnetic regime, we can conclude that there are significant contributions from local moments.

Our most direct evidence for local moments comes from the temperature regime below the spin-ordering transition that has been characterized by neutron diffraction.[16–18] There we see an evolution of the anisotropic susceptibility that can be simply interpreted in terms of the classic expectations for a noncollinear antiferromagnet (see Fig. 1). Furthermore, on following the magnetization vs applied field, we find evidence for a spin-flop transition at $H=6$ T. Such a transition is consistent with an anisotropy of the superexchange interaction between local moments.

To describe the doping dependence of the susceptibility of polycrystalline $La_{2-x}Sr_xCuO_4$, Johnston[6] proposed that there should be a component χ^{Cu} due to antiferromagnetically coupled local moments. Furthermore, he assumed that it had the form $\chi^{Cu}_{max}(x)f(T/T_{max})$, where f is a normalized "universal" function and T_{max} is a function of x. He found that he could get a good fit to the data if he included a temperature-independent component with a magnitude roughly proportional to x. The same scaling analysis was later applied to a more extensive set of measurements by Nakano *et al.*[7] The temperature-independent component is generally assumed to correspond to the Pauli susceptibility, χ^P, associated with the doped carriers.

This successful, but *ad hoc*, decomposition has been widely applied, and we initially attempted to use it on our own results to separate out the contribution from local moments. We found, however, that a χ^P component of the commonly accepted magnitude is not compatible with the large anisotropy observed in the single-crystal data. We have strengthened our case by extending the analysis to include data for $La_{2-x}Ba_xCuO_4$ with $x=0.095$ and 0.155. We con-

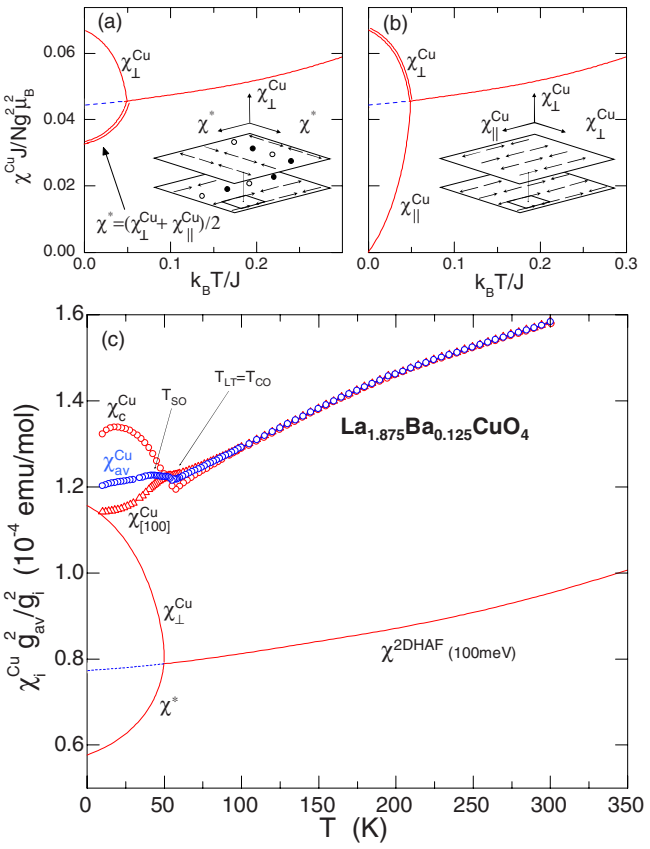

FIG. 1. (Color online) Schematic of χ^{Cu} vs T for (a) the stripe phase, and (b) a collinear AF order. (- - -) χ^{Cu} in the absence of order. (c) $\chi_c^{Cu} g_{av}^2/g_c^2$, $\chi_{[100]}^{Cu} g_{av}^2/g_{ab}^2$, and $\chi_{av}^{Cu}=\frac{2}{3}\chi_{[100]}^{Cu} g_{av}^2/g_{ab}^2 + \frac{1}{3}\chi_c^{Cu} g_{av}^2/g_c^2$ for $La_{1.875}Ba_{0.125}CuO_4$. T_{LT} marks LTO↔LTT transition, T_{SO} and T_{CO} the spin and charge stripe order. Lines show χ^{2DHAF} for $J=100$ meV, including schematic dependence in ordered phase.

clude that any temperature-independent χ^P component must be an order of magnitude smaller than that reported in Refs. 6 and 7.

As a result of the much reduced χ^P, the extracted χ^{Cu} is larger at low temperature than previously assumed. Based on our insights, we discuss the implications for the evolution of magnetic correlations in $La_{2-x}Sr_xCuO_4$ and $La_{2-x}Ba_xCuO_4$ vs doping and temperature. In particular, we show that the maximum of $\chi^{Cu}(T)$, which occurs at $T_{max}(x)$, is inversely proportional to the effective superexchange energy J determined by Raman and neutron scattering.

The rest of this paper is organized as follows. Section II describes the experimental methods. In Sec. III, we present the data and work step-by-step through the analysis. The implications are discussed in Sec. IV, and a brief conclusion is given in Sec. V.

II. EXPERIMENTAL METHODS

The $La_{1.875}Ba_{0.125}CuO_4$ crystal studied here, with a mass of 0.6 g, was cut from the same single-crystal rod grown by the traveling-solvent floating-zone method that was the source of samples for previous work.[17–19] For the complementary measurements on $x=0.095$ and $x=0.155$, similarly sized crystals were used. The magnetization M was measured with a superconducting quantum interference device (SQUID) magnetometer at Brookhaven ($H_{max}=7$ T), and a vibrating sample magnetometer at IFW-Dresden ($H_{max}=15$ T). In the case of $La_{1.875}Ba_{0.125}CuO_4$, $\chi=M/H$ was recorded for $\mathbf{H}\|[001]$ (c axis) as well as $\mathbf{H}\|[100]$, [010] and [110] (ab plane) in zero-field-cooled (ZFC) and field-cooled (FC) modes. [See the high-temperature-tetragonal (HTT) unit cell in Fig. 2(b) for definition of directions.] Measurements of $\chi_{[100]}$ and $\chi_{[010]}$ produce identical results, while $\chi_{[110]}$ shows clear distinctions. Bulk superconductivity (SC) in this sample appears below ~2.3 K in $H=20$ G. SC fluctuations are detectable up to ~40 K for $\mathbf{H}\|\mathbf{c}$,[18,19] but are suppressed down to ~20 K (~5 K) by a field of 2 T (7 T).

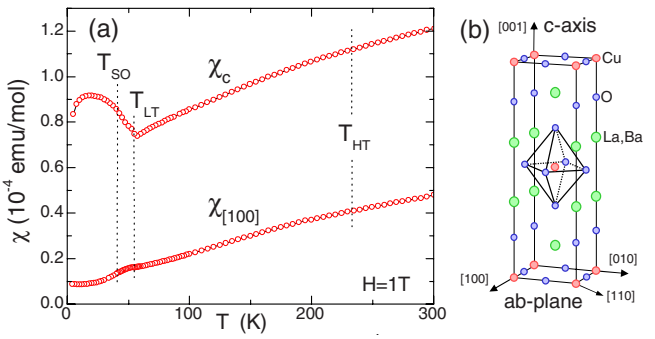

FIG. 2. (Color online) (a) χ obtained in FC mode with $H=1$ T applied along [100] and [001] in $La_{1.875}Ba_{0.125}CuO_4$. (b) HTT unit cell with definition of directions.

III. DATA AND ANALYSIS

Figure 2(a) shows the raw FC data for χ_c and $\chi_{[100]}$ in $La_{1.875}Ba_{0.125}CuO_4$. While there is no signature of the 235 K structural transition (T_{HT}) from the HTT to the low-temperature-orthorhombic (LTO) phase, there are clear changes at $T_{LT}=54.5$ K, where the crystal transforms into the low-temperature tetragonal (LTT) phase.[18,20] We know that charge-stripe order sets in at T_{LT}.[16,18,19,21,22] χ_c increases rapidly below T_{LT} and is independent of the magnetic field [except at low T, due to diamagnetism from SC fluctuations; see Fig. 3(c) and Ref. 19]. In contrast, $\chi_{[100]}$ only shows a small step at T_{LT}, followed by a significant decrease below 42 K. This decrease is not due to diamagnetism from SC, but is connected to the onset of spin stripe order at T_{SO}, as detected by μSR (Ref. 23) and neutron diffraction.[16,18] Below $H\sim0.5$ T, T_{SO} is marked by a clear kink in $\chi_{[100]}$ and $\chi_{[110]}$, as is shown in the insets of Fig. 3 as well as in Ref. 19.

A. Contributions to the measured susceptibility

The measured susceptibility $\chi_i(T)$ ($i=c,ab$) can be written as

$$\chi_i(T) = \chi_i^s(T) + \chi^{core} + \chi_i^{VV}. \quad (1)$$

The core diamagnetism χ^{core} amounts to -1.01×10^{-4} emu/mol, as determined from standard tables.[24] The

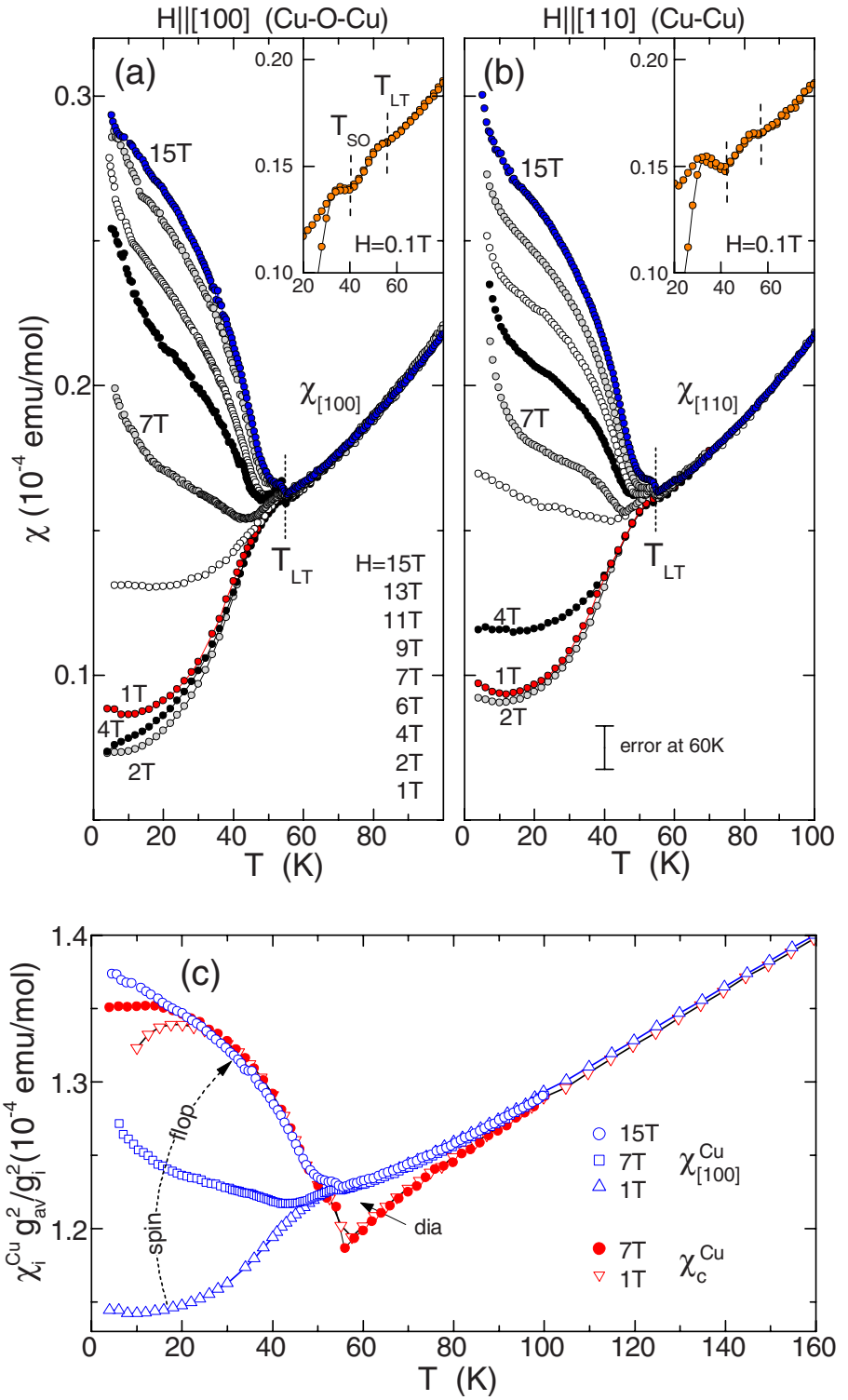

FIG. 3. (Color online) χ of $La_{1.875}Ba_{0.125}CuO_4$ obtained in FC mode (a) for $\mathbf{H}\|[100]$ and (b) for $\mathbf{H}\|[110]$. Small deviations between curves (within error bar at bottom) for different fields and magnetometers due to experimental error were corrected by shifts in χ so that curves match for $T>T_{LT}$ where no field dependence was observed. Insets: FC and ZFC data for $H=0.1$ T showing clear kinks at T_{SO} and T_{LT}. (c) Comparison of the field dependence of $\chi_i^{Cu} g_{av}^2/g_i^2$.

Van Vleck susceptibility of the Cu^{2+} ions, χ_i^{VV}, depends on the direction of the field, but is independent of temperature; we will come back to it shortly. We can write the spin contribution as

$$\chi_i^s(T) = \chi_i^{Cu}(T) + \chi^P. \quad (2)$$

Here χ_i^{Cu} is the contribution from local moments,[1]

TABLE I. Parameters from analysis of χ_i^s for different cases, as discussed in the text. Bold numbers indicate parameters that were varied during fit. Numbers in the first row result from individual fit for crystal with $x=0.125$; see Fig. 1(c). In contrast, the data in rows I–IV were obtained by simultaneous fits for all x; see Figs. 7(b)–7(d). Susceptibilities are given in units of 10^{-4} emu/mol. R is the sum of squared differences.

Case	$\chi^P_{x=0.095}$	$\chi^P_{x=0.125}$	$\chi^P_{x=0.155}$	χ^{VV}_{ab}	χ^{VV}_{c}	g_{ab}	g_c	R
0		0		**0.09**	**0.28**	**2.19**	**2.58**	**0.005**
I	0	0	0	**0.11**	**0.33**	**2.18**	**2.56**	**0.16**
II	0.3	0.3	0.3	**0.18**	**0.54**	**2.18**	**2.56**	**0.16**
III	0.66	0.89	1.13	0.11	0.33	**2.58**	**3.74**	**36**
IV	0.66	0.89	1.13	**0.35**	**1.04**	**2.03**	**2.10**	**9.4**

$$\chi_i^{Cu} = \frac{Ng_i^2\mu_B^2}{kT}\sum_{\mathbf{r}}\langle S_{\mathbf{0}}^i S_{\mathbf{r}}^i\rangle, \tag{3}$$

where N is the density of Cu atoms, $S_{\mathbf{r}}^i$ is the spin component in direction i for the Cu atom at site $\mathbf{r}$; in the paramagnetic phase, χ_i^{Cu} remains anisotropic, as g_{ab} and g_c typically differ by 15% for Cu^{2+} compounds.[25] The isotropic Pauli susceptibility can be expressed as[26]

$$\chi^P = (g\mu_B/2)^2\rho(\epsilon_F), \tag{4}$$

where $g\approx 2$ and $\rho(\epsilon_F)$ is the electronic density of states at the Fermi energy ϵ_F. (In principle, the paramagnetic response of conduction electrons due to their spins is partially offset by their orbital response, in the form of Landau diamagnetism.) For a Fermi liquid, the density of states is independent of temperature, so that χ^P is a constant. As the cuprates do not follow conventional Fermi-liquid behavior,[8,10,27] χ^P might be temperature dependent.

In simple metals, such as Na or Al, all of the spin response comes from delocalized conduction electrons. The doped cuprates are unusual metals, but one can nevertheless consider the extent to which the charge carriers also determine the magnetic response. Thus, we start our analysis with the following question: can we explain all of the temperature dependence in our single-crystal $\chi_i(T)$ simply in terms of $\chi^P(T)$?

To answer this, we consider the anisotropy between $\chi_{ab}(T)$ and $\chi_c(T)$. From Eqs. (1) and (2), we see that there are two sources of anisotropy, χ_i^{VV} and χ_i^{Cu}. Looking at Fig. 2(a), we see that $\chi_c-\chi_{[100]}$ varies with temperature over the entire measurement range, and especially below T_{SO}. As noted above, the Van Vleck component is temperature independent, and hence the temperature-dependent anisotropy must come from the local-moment contribution. Thus, we immediately conclude that the temperature dependence of the spin susceptibility cannot come uniquely from a temperature dependence of the electronic density of states.

B. Initial analysis of anisotropy

In principle, we can determine χ_i^{Cu} from the anisotropy of the measured susceptibility; however, to do this, we need to know the values of χ_i^{VV} and the g_i factors. For isolated Cu^{2+} ions, one has

$$\chi_c^{VV} = 8\mu_B^2/\epsilon_0, \tag{5}$$

$$\chi_{ab}^{VV} = 2\mu_B^2/\epsilon_1, \tag{6}$$

$$g_c = 2 + 8\lambda/\epsilon_0, \tag{7}$$

$$g_{ab} = 2 + 2\lambda/\epsilon_1, \tag{8}$$

where λ is the spin-orbit coupling, and the energies ϵ_0 and ϵ_1 are the crystal-field splittings between the $3d_{x^2-y^2}$ and the tetragonally-split t_{2g} orbitals.[25,28] In the CuO_2 planes, the $3d$ states turn into bands, and one must average over the Brillouin zone to properly evaluate these quantities. The only calculation[29] of such factors for cuprates that we know of was performed for hypothetical Sc_2CuO_4. While we cannot apply those results directly to our case, we can use them as guidance.

We find that we must resort to fitting the data in order to determine the anisotropy factors. To do so, we will first consider the case $\chi^P=0$; we will later come back to consider the impact of a finite χ^P. From Eqs. (1)–(3), we find that, in the paramagnetic regime,

$$\chi_{ab}^{Cu}/g_{ab}^2 = \chi_c^{Cu}/g_c^2, \tag{9}$$

or, equivalently,

$$(\chi_{ab} - \chi^{core} - \chi_{ab}^{VV})/g_{ab}^2 = (\chi_c - \chi^{core} - \chi_c^{VV})/g_c^2. \tag{10}$$

Thus, we must vary the anisotropic factors in order to get a unique χ_i^{Cu}/g_i^2 from the experimentally measured χ_{ab} and χ_c. We note from Eqs. (5)–(8) that

$$(g_c-2)/(g_{ab}-2) = \chi_c^{VV}/\chi_{ab}^{VV} = \gamma, \tag{11}$$

where one expects $\gamma\leq 4$.[28] The analysis is relatively insensitive to the precise value of γ, so we reduce the number of adjustable parameters to two by setting $\gamma=3$, approximately equal to the ratio calculated for Sc_2CuO_4.[29] Applying the analysis to the temperature range $100\ \mathrm{K}\leq T\leq 300\ \mathrm{K}$, we obtain $g_{ab}=2.19$, $g_c=2.58$, $\chi_{ab}^{VV}=0.09\times10^{-4}$ emu/mol and $\chi_c^{VV}=0.28\times10^{-4}$ emu/mol (see top row of Table I), as well as the polycrystalline averages $g_{av}=2.32$ and $\chi_{av}^{VV}=0.15\times10^{-4}$ emu/mol. Finally, the results obtained for $\chi_c^{Cu}g_{av}^2/g_c^2$ and $\chi_{[100]}^{Cu}g_{av}^2/g_{ab}^2$ are plotted in Figs. 1(c) and 3(c).

Our fitted values for the Van Vleck susceptibilities are quite comparable to the theoretical results[29] of $\chi_{ab}^{VV}=0.15\times10^{-4}$ emu/mol and $\chi_c^{VV}=0.4\times10^{-4}$ emu/mol. We note that considerably larger values for Van Vleck susceptibilities have been reported;[30,31] however, those studies did not in-

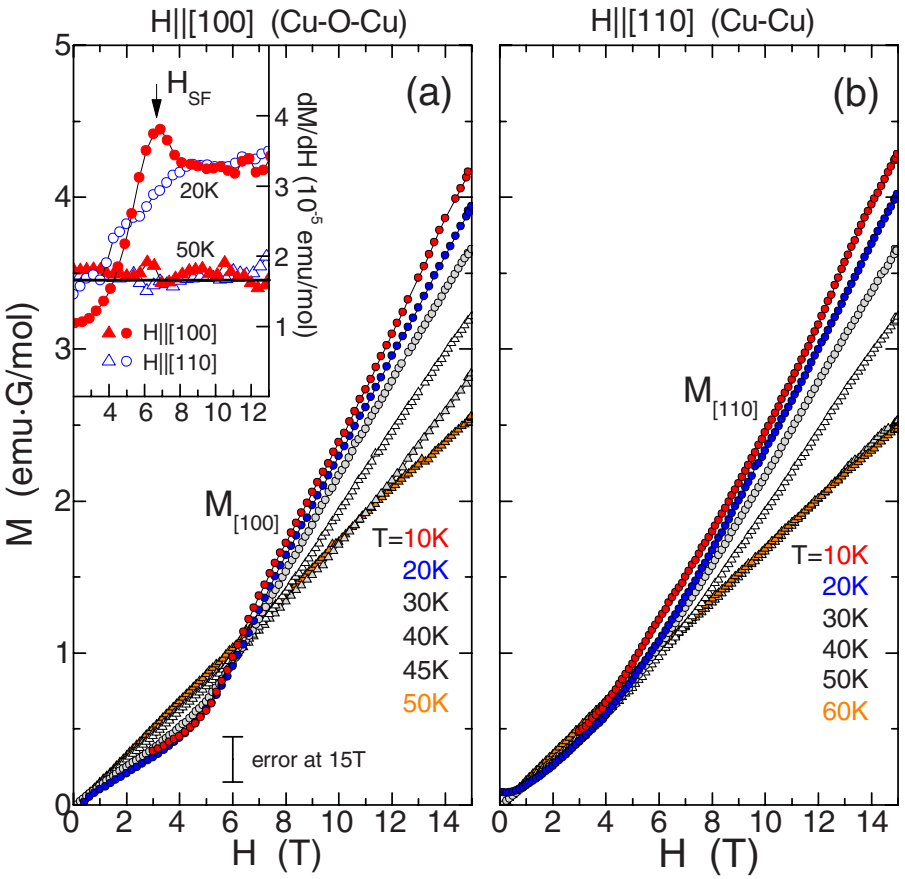

FIG. 4. (Color online) $M(H)$ of $La_{1.875}Ba_{0.125}CuO_4$ obtained in ZFC mode (a) for $\mathbf{H}\|[100]$ and (b) for $\mathbf{H}\|[110]$. Small experimental errors were corrected so that at 15 T M/H is consistent with χ in Fig. 3 (see error bar). For the 10 K curve, the data is limited to $H>3$ T to avoid effects of superconductivity at lower fields. Inset: derivative dM/dH, calculated after three-point averaging of $M(H)$ (except for $T=20$ K with $\mathbf{H}\|[100]$, where two-point averaging was used due to the larger point spacing).

clude the possibility of anisotropy in χ_i^{Cu}. In fact, we will reproduce this effect in Sec. III F.

C. Spin anisotropy in the ordered state

Let us consider how the anisotropy is connected with the spin ordering. In the classic case of collinear antiferromagnetic (AF) order, Fig. 1(b), one measures $\chi_\parallel^{Cu}$ for $\mathbf{H}\|\mathbf{S}$ and $\chi_\perp^{Cu}$ for the two orthogonal orientations; $\chi_\parallel^{Cu}\to 0$ as $T\to 0$,[1] while $\chi_\perp^{Cu}$ grows relative to the paramagnetic state. In contrast, for $La_{1.875}Ba_{0.125}CuO_4$ χ_c^{Cu} behaves like $\chi_\perp^{Cu}$, but $\chi_{[100]}^{Cu}$ and $\chi_{[010]}^{Cu}$ each seem to correspond to $\frac{1}{2}(\chi_\parallel^{Cu}+\chi_\perp^{Cu})$, as indicated in Fig. 1(a). This anisotropy is consistent with the stripe model. The stripes rotate by $\pi/2$ from one layer to the next, following the crystalline anisotropy,[32] and the effective spin anisotropy should rotate as well, with the Cu spins ordering within the *ab* plane.[33] (Note that twinning could also yield the same average noncollinear response for a completely collinear AF.)

D. Spin-flop transition

Next, consider the field dependence of $\chi_{[100]}$ shown in Fig. 3(a). Increasing the field above 4 T causes $\chi_{[100]}$ to rapidly increase for $T\lesssim 40$ K; when $H=15$ T, $\chi_{[100]}^{Cu}(g_{av}^2/g_{ab}^2)$ matches $\chi_c^{Cu}(g_{av}^2/g_c^2)$. This behavior is consistent with a spin-flop in the spin stripes. The spin-flop transition is clearly seen in the $M_{[100]}(H)$ curves of Fig. 4(a). $M_{[100]}$ becomes nonlinear for $T<50$ K, with the transition marked by a peak in $dM_{[100]}/dH$ at $H_{SF}\sim 6$ T, as shown in the inset. Similar data for $\chi_{[110]}$ in Fig. 3(b) and $M_{[110]}$ in Fig. 4(b) exhibit a much broader transition with no peak in $dM_{[110]}/dH$ [see inset of Fig. 4(a)]. The anisotropy in dM/dH implies that the spins that flop at the transition initially have $\mathbf{S}\|[100]$. Figure 5 illustrates the situation. At zero field, we presume that $\mathbf{S}\|[010]$ in plane $z=0$, and $\mathbf{S}\|[100]$ in plane $z=0.5$. For $H>H_{SF}$ along [100], spins in plane $z=0.5$ flop so that the staggered moments are approximately perpendicular to the field [Fig. 5(b)]. It is the gain in Zeeman energy, by slightly polarizing the spins in the field direction, that stabilizes the flopped state. When applying $\mathbf{H}\|[110]$, spins in all planes continuously rotate until the staggered moment again is perpendicular to $\mathbf{H}$ [Fig. 5(c)], so there is no sharp transition.

Figure 6 shows the resulting phase diagram for $\mathbf{H}\|[100]$. The LTO$\leftrightarrow$LTT transition at T_{LT} is field independent, while the onset of spin stripe order shifts from $T_{SO}=42(3)$ K at 0.1 T to 49(3) K at 15 T. X-ray diffraction data indicate that charge stripes order at $T_{CO}=T_{LT}$.[18,21,22] Hence, for $T_{SO}<T<T_{CO}$ there are static charge stripes but no static spin stripes, which is consistent with recent inelastic neutron-scattering

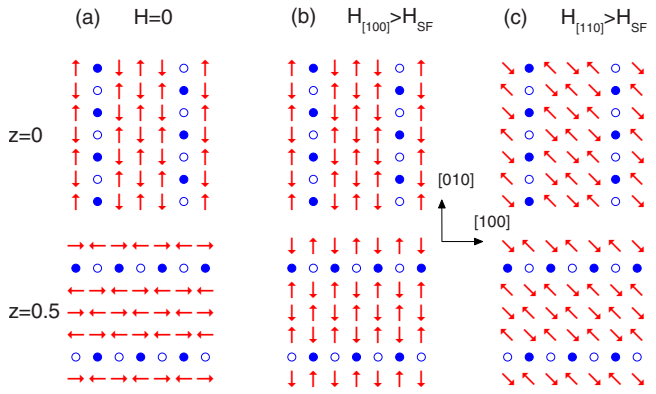

FIG. 5. (Color online) Model for spin structure of site-centered stripes as a function of field. (●,○) Half-filled charge stripes. Stripes in adjacent planes at $z=0$ and 0.5 are perpendicular. (a) Spin structure for $H=0$, (b) $\mathbf{H}\|[100]$, and (c) $\mathbf{H}\|[110]$.

results indicating the opening of a spin-wave gap only for $T \lesssim T_{SO}$.[18] On the other hand, χ_c increases right at T_{CO}, which suggests that spins become parallel to the CuO_2 planes; see Fig. 2(a). This means that below T_{CO} spin dimensionality is effectively reduced from 2D-Heisenberg to 2D-*XY*. (Exchange anisotropy becomes relevant even in the absence of static order.) This is extremely interesting because a 2D-*XY* system allows for topological order without additional anisotropies or interlayer coupling, with 2D SC being one possibility.[18,19,34] Finally, Fig. 6 indicates the spin-flop transition for $T<T_{SO}$. H_{SF} is of the same magnitude as in the LTT phase of antiferromagnetic $La_{1.8}Eu_{0.2}CuO_4$,[35] suggesting that the in-plane gap has changed only moderately.

E. Diamagnetism in paramagnetic state

The reader may already have noted in Fig. 3(c) the apparent anisotropy at $T \gtrsim 54$ K, where $\chi_c^{Cu} g_{av}^2/g_c^2 < \chi_{[100]}^{Cu} g_{av}^2/g_{ab}^2$. This behavior does not make sense in terms of exchange anisotropy. Instead, we believe that χ_c^{Cu} bears a weak two-dimensional diamagnetic contribution associated with the vortex liquid state proposed by Li *et al.*,[36] based on magnetization measurements on $La_{2-x}Sr_xCuO_4$ for $0.03 \le x \le 0.07$. Similar behavior appears above T_c at other compositions of $La_{2-x}Ba_xCuO_4$. Examples for $x=0.095$ and 0.155 can be seen in Fig. 7

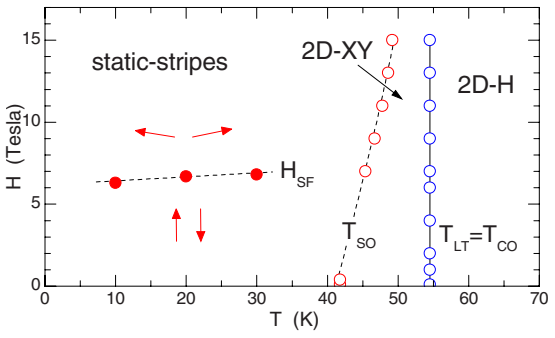

FIG. 6. (Color online) *H-T* diagram of $La_{2-x}Ba_xCuO_4$ as determined for $\mathbf{H}\|[100]$. Only for $H \lesssim 0.5$ T and $H \gtrsim 7$ T an anomaly at T_{SO} is observed. For SC properties see Ref. 19.

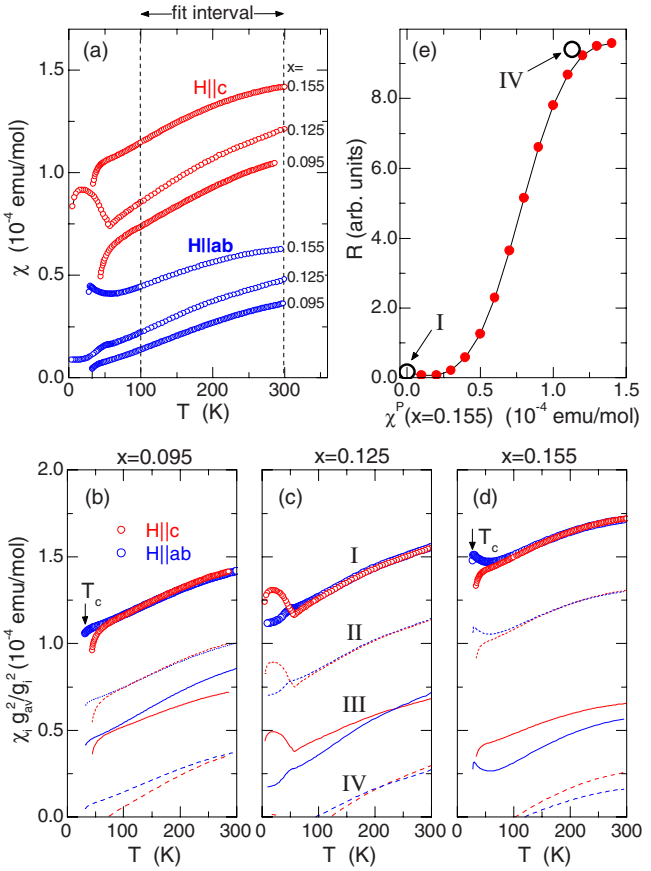

FIG. 7. (Color online) (a) $\chi_i(T)$ of $La_{2-x}Ba_xCuO_4$ for different dopings $x=0.095$, 0.125, and 0.155. Note that the crystals with $x=0.095$ and 0.155 are bulk superconductors with $T_c=32$ K and 30 K, respectively. [(b)–(d)] Spin susceptibility $\chi_i^{Cu}(T)(g_{av}^2/g_i^2)$ extracted from data in (a) under different conditions, as discussed in the text. Roman numbers I–IV refer to corresponding parameter sets in Table I. (e) Least-squared deviation R vs χ^P at $x=0.155$ doping for fits in which a linear x dependence of $\chi^P(x)$ is assumed. Open circles indicate R values for cases I and IV from Table I.

F. Anisotropy and doping dependence of susceptibility

Now we will reconsider our initial assumption that $\chi^P=0$. Obviously, that assumption is in conflict with the scaling analysis,[6,7,31] which gives approximately $\chi^P \sim x$. To properly evaluate the latter form, we need to jointly analyze anisotropic measurements for samples with different hole contents. In Fig. 7(a) we show the raw data of χ_i on single crystals of $La_{2-x}Ba_xCuO_4$ with compositions from $x=0.095$ to 0.155. Keeping in mind that χ_i^{VV} and g_i should be independent of doping, we now repeat our fitting of these parameters for all three samples simultaneously and with various choices for χ^P. These choices and the fitted parameter values are listed in Table I, and the best-fit results for χ_i^{Cu} are plotted in Figs. 7(b)–7(d). The quality of fit parameter R is equal to the sum of the squared differences between the two versions of $\chi_i^{Cu}(g_{av}^2/g_i^2)$, with $H\|ab$ and $H\|c$, evaluated over the fit interval of 100 K $\le T \le$ 300 K.

Case I corresponds to $\chi^P=0$, and clearly it gives an excellent match of $\chi_i^{Cu}(g_{av}^2/g_i^2)$ for all three compositions. The fitted parameters are quite close to what we obtained for x

=0.125 alone (case 0). For cases III and IV, we fix $\chi^P(x)$ to values interpolated from results in Refs. 6, 7, and 37. In case III, we use the χ_i^{VV} of case I and only vary the g_i, while all parameters are varied for case IV. In both, the matching is very poor. In fact, for case IV the resulting $\chi_i^{Cu}(g_{av}^2/g_i^2)$ becomes negative as a result of the large anisotropy in χ_i^{VV} that is required to compensate for the reduced magnitude of $\chi_i^{Cu}(g_{av}^2/g_i^2)$. With reduced values of χ_i^{VV}, as in case III, the g_i factors become unreasonably large.

It is important to note that the analysis is insensitive to a doping-independent but finite χ^P. Although unphysical, we present this situation in case II, which demonstrates a match of equal quality to case I. We include this case simply to show a limitation in terms of uniqueness of our analysis.

While the values of $\chi^P(x)$ inferred from Refs. 6, 7, and 37 clearly seem to be unreasonable when anisotropy is taken into account, it is still possible that there is a $\chi^P(x)$ contribution of smaller magnitude. Hence, we have performed fits allowing $\chi^P(x) \sim x$ with a variable scale factor. Figure 7(e) shows R as a function of the corresponding $\chi^P(x=0.155)$. We see that R strongly increases for $\chi^P(x=0.155) \gtrsim 0.25 \times 10^{-4}$ emu/mol, which is a limit nearly five times smaller than the value given by the scaling analysis (see case IV in Table I). We conclude that if a temperature-independent contribution from mobile carriers is present, it must be an order of magnitude smaller than the estimates based on the scaling analysis of the static magnetic susceptibility.

IV. DISCUSSION

Our analysis indicates that the bulk spin susceptibility χ^s in $La_{1.875}Ba_{0.125}CuO_4$ comes dominantly from local Cu moments and that χ^P does not make a substantial contribution. In Fig. 1(c), we compare our results for χ^{Cu} with the prediction for the two-dimensional Heisenberg antiferromagnet (2DHAF) with $J=100$ meV, where the estimate for J is taken from a neutron-scattering study of the magnetic excitation spectrum.[17] A clear implication of our analysis is that χ^s of the doped cuprate is greater than that of the undoped antiferromagnet. A comparison of the anisotropy below T_{SO} suggests a substantial ordered moment, as found by muon spin-rotation studies.[23,38] If we estimate $\chi_\parallel^{Cu}$ as

$$\chi_\parallel^{Cu} = 2\chi_{[100]}^{Cu}(g_{av}^2/g_{ab}^2) - \chi_c^{Cu}(g_{av}^2/g_c^2), \tag{12}$$

then it appears that $\chi_\parallel^{Cu}$ remains finite at low temperature, in contrast to the expectation $\chi_\parallel^{Cu} \to 0$ for an undoped antiferromagnet. The lack of perfect spin ordering was already indicated by a Cu nuclear quadrupole resonance (NQR) study,[39] where attempts to measure the antiferromagnetic resonance at temperatures down to 0.35 K provided evidence for a broad distribution of hyperfine fields at the Cu site (averaged over the NQR time scales).

For another comparison, Fig. 8 shows χ_{av}^{Cu} data for polycrystalline $La_{2-x}Sr_xCuO_4$ with $x=0.08$ and 0.15, extracted from the bulk susceptibility using the same values for the core diamagnetism and Van Vleck susceptibility as for the $La_{1.875}Ba_{0.125}CuO_4$ result, which is shown as a polycrystalline average. We note that the $La_{2-x}Ba_xCuO_4$ result is consistent with the $La_{2-x}Sr_xCuO_4$ data both in magnitude and in terms of the trend of increasing χ_{av}^{Cu} with doping. We note that the latter observation is contrary to what has been inferred based on the scaling analysis.[7,8]

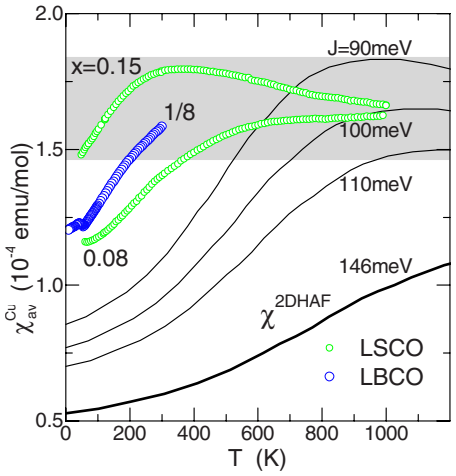

FIG. 8. (Color online) χ_{av}^{Cu} vs T for the $La_{1.875}Ba_{0.125}CuO_4$ single crystal and for polycrystalline $La_{2-x}Sr_xCuO_4$ (Ref. 40). Solid lines correspond to χ^{2DHAF} for different J (Ref. 1).

In Fig. 8, we also compare calculations for the 2DHAF with different values of J. As one can see, χ^{2DHAF} provides a reasonable estimate of $\chi_{max}^{Cu}=\chi^{Cu}(T_{max})$ for an appropriate J, but gives poor agreement for the temperature T_{max} at which χ^{Cu} reaches its maximum. Now, we know from neutron-scattering studies that doping significantly modifies the dynamic spin correlations from those of the undoped insulator,[17,41–44] so it should not be surprising that T_{max} would be reduced from that of a spin-only model system. On the other hand, χ_{max}^{Cu} might be less affected, as it corresponds to the response as antiferromagnetic correlations just begin to overcome disturbances from thermal or electron-scattering excitations. Indeed, Imai *et al.*[45] concluded quite some time ago, on the basis of NQR measurements of the ^{63}Cu nuclear spin-lattice relaxation rate, that the Cu spin correlations in $La_{2-x}Sr_xCuO_4$ are independent of doping at high temperatures.

Johnston[1] has collected analytical results for a wide range of low-dimensional Heisenberg models (with only nearest-neighbor coupling) and has shown that χ_{max}^{Cu} has the general form

$$\chi_{av}^{Cu}(T_{max}) = \left(\frac{A}{2z_{eff}J}\right) N g_{av}^2 \mu_B^2, \tag{13}$$

where z_{eff} is the effective number of nearest neighbors and A is a scale factor that ranges from 0.4 for a system of spin dimers ($z_{eff}=1$) to 0.75 for a 2D square lattice ($z_{eff}=4$). Thus, if z_{eff} does not change much with doping, we might expect χ_{max}^{Cu} to vary as N_{eff}/J, where $N_{eff}=(1-x)N$ and N is the density of Cu atoms.

In Fig. 9, we plot χ_{max}^{Cu} extracted from the literature[6,7,37,40] and analyzed with our scheme. For comparison, we have used Eq. (13), with $z_{eff}=4$ and J taken from neutron[17,41,42] and Raman[46] studies, to estimate χ_{max}^{Cu}. For the case $\chi^P=0$, the experimental and calculated trends for χ_{max}^{Cu} are quite

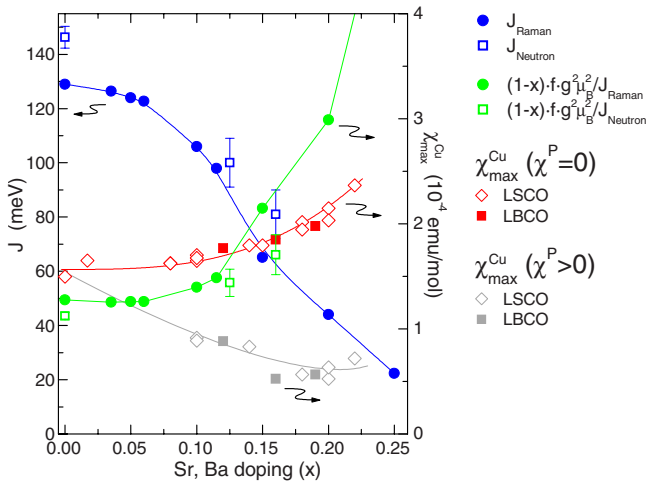

FIG. 9. (Color online) Comparison of experimental (Refs. 6, 7, 37, and 40) $\chi^{Cu}_{av}(T_{max})$ (evaluated with our χ^{VV}_{av}) and values calculated from experimental J values (Refs. 17, 41, 42, and 46) [with $f=(A/2z_{eff})N=0.094N$ for $z_{eff}=4$], as discussed in the text.

similar across the underdoped regime. Clear deviations appear as x crosses into the overdoped regime. Of course, $T_{max}\rightarrow 0$ for $x\sim 0.22$,[7,37] suggesting that we get to a point beyond which dominant antiferromagnetic correlations never fully develop. [However, $\chi(T)$ remains temperature dependent at high doping, and at least up to $x\sim 0.3$ does not demonstrate the temperature-independent behavior expected for a conventional metal.[47]] Our interpretation is consistent with neutron-scattering observations of a rapid fall off in the weight of antiferromagnetic spin fluctuations with overdoping.[48,49] For comparison, we also show the case $\chi^{Cu}_{max}=\chi^{s}_{max}-\chi^{P}$ obtained from the scaling analysis,[6,7,37] which is clearly inconsistent with our expectation based on Eq. (13).

The developing picture in underdoped cuprates is one of considerable incoherence of the electronic correlations at high temperatures.[50] Optical conductivity studies of $La_{2-x}Sr_xCuO_4$, $La_{2-x}Ba_xCuO_4$, and $YBa_2Cu_3O_{6+x}$ indicate that the Drude peak, often taken as an indication of coherent behavior, disappears as the temperature is increased toward the pseudogap crossover temperature, T^*.[51–53] A recent analysis[54] of temperature- and doping-dependent Hall-effect measurements[55] suggests that not only the doped holes but also thermally activated carriers participate in the transport at high temperature. It has been noted[54,56] that T^* identified from transport properties is quite close to T_{max} from the bulk susceptibility. Thus, it appears that the coherent nodal metallic states[53] and the antiferromagnetic spin correlations develop together on cooling below T^*. This coevolution is compatible with the development of stripe correlations,[57] as suggested by neutron-scattering studies.[16,58,59]

There have been suggestions that the pseudogap might be the consequence of spin-density-wave (SDW) correlations.[60,61] In that case, the magnetic response would come dominantly from the charge carriers. This possibility now seems unlikely, as we have argued that the static susceptibility is dominated by the response of local moments, and there is no evidence of coherent electronic states at $T\gtrsim T^*$ from which a SDW might develop.

Finally, our interpretation of the static susceptibility is compatible with the distinct dynamic responses detected by nuclear magnetic resonance studies[62,63] at Cu and O in-plane sites in $La_{2-x}Sr_xCuO_4$. The site-dependent responses can be understood in terms of the spatial inhomogeneity associated with stripe correlations.[64–68] By symmetry, the O site does not see the spins on the two nearest-neighbor Cu sites in the uniform antiferromagnetic state; however, stripe correlations can break this symmetry, allowing O to detect the spin susceptibility. In fact, it is the existence of the stripe correlations that allows for the coexistence of regions of antiferromagnetically coupled Cu moments and mobile charge carriers.[18,57]

V. CONCLUSION

To conclude, we have presented evidence that the bulk susceptibility in underdoped and optimally doped $La_{2-x}(Sr,Ba)_xCuO_4$ is dominated by the response of antiferromagnetically coupled Cu moments, with little contribution from free carriers. This conclusion has implications for the interpretation of the dynamic magnetic susceptibility. If electronic quasiparticles were to contribute significantly to the dynamic susceptibility through Fermi-surface-nesting effects, then one would expect an associated contribution to the static susceptibility. The absence of a substantial isotropic component of electronic origin in χ^s raises questions about the relative importance of quasiparticle contributions to the dynamic susceptibility in underdoped cuprates.

ACKNOWLEDGMENTS

We acknowledge valuable discussions with F. H. L. Essler, J. P. Hill, S. A. Kivelson, A. Savici, A. M. Tsvelik, and I. Zaliznyak. M.H. is grateful to B. Büchner, H. Grafe, I. Kiwitz, R. Klingeler, and N. Tristan for help during the experiment at the IFW-Dresden. This work was supported by the Office of Science, U.S. Department of Energy under Contract No. DE-AC02-98CH10886.

[1] D. C. Johnston, in *Handbook of Magnetic Materials*, edited by K. H. J. Buschow (Elsevier Science, New York, 1997), Vol. 10.
[2] H. Alloul, T. Ohno, and P. Mendels, Phys. Rev. Lett. **63**, 1700 (1989).
[3] S. Hüfner, M. A. Hossain, A. Damascelli, and G. A. Sawatzky, Rep. Prog. Phys. **71**, 062501 (2008).
[4] P. A. Lee, Rep. Prog. Phys. **71**, 012501 (2008).
[5] P. W. Anderson, *The Theory of Superconductivity in the High-T_c Cuprates* (Princeton University, Princeton, NJ, 1997), pp. 98–99.

[6] D. C. Johnston, Phys. Rev. Lett. **62**, 957 (1989).
[7] T. Nakano, M. Oda, C. Manabe, N. Momono, Y. Miura, and M. Ido, Phys. Rev. B **49**, 16000 (1994).
[8] P. A. Lee, N. Nagaosa, and X.-G. Wen, Rev. Mod. Phys. **78**, 17 (2006).
[9] V. Barzykin and D. Pines, Phys. Rev. Lett. **96**, 247002 (2006).
[10] T. Timusk and B. Statt, Rep. Prog. Phys. **62**, 61 (1999).
[11] N. Bulut, D. Hone, D. J. Scalapino, and N. E. Bickers, Phys. Rev. Lett. **64**, 2723 (1990).
[12] J. P. Lu, Q. Si, J. H. Kim, and K. Levin, Phys. Rev. Lett. **65**, 2466 (1990).
[13] P. B. Littlewood, J. Zaanen, G. Aeppli, and H. Monien, Phys. Rev. B **48**, 487 (1993).
[14] V. J. Emery, S. A. Kivelson, and H. Q. Lin, Phys. Rev. Lett. **64**, 475 (1990).
[15] V. J. Emery and S. A. Kivelson, Physica C **209**, 597 (1993).
[16] M. Fujita, H. Goka, K. Yamada, J. M. Tranquada, and L. P. Regnault, Phys. Rev. B **70**, 104517 (2004).
[17] J. M. Tranquada, H. Woo, T. G. Perring, H. Goka, G. D. Gu, G. Xu, M. Fujita, and K. Yamada, Nature (London) **429**, 534 (2004).
[18] J. M. Tranquada, G. D. Gu, M. Hücker, Q. Jie, H.-J. Kang, R. Klingeler, Q. Li, N. Tristan, J. S. Wen, G. Y. Xu, Z. J. Xu, J. Zhou, and M. v. Zimmermann, Phys. Rev. B **78**, 174529 (2008).
[19] Q. Li, M. Hucker, G. D. Gu, A. M. Tsvelik, and J. M. Tranquada, Phys. Rev. Lett. **99**, 067001 (2007).
[20] J. D. Axe, A. H. Moudden, D. Hohlwein, D. E. Cox, K. M. Mohanty, A. R. Moodenbaugh, and Y. Xu, Phys. Rev. Lett. **62**, 2751 (1989).
[21] P. Abbamonte, A. Rusydi, S. Smadici, G. D. Gu, G. A. Sawatzky, and D. L. Feng, Nat. Phys. **1**, 155 (2005).
[22] M. v. Zimmermann, R. Nowak, G. D. Gu, C. Mennerich, H.-H. Klauss, and M. Hücker, Rev. Sci. Instrum. **79**, 033906 (2008).
[23] G. M. Luke, L. P. Le, B. J. Sternlieb, W. D. Wu, Y. J. Uemura, J. H. Brewer, T. M. Riseman, S. Ishibashi, and S. Uchida, Physica C **185-189**, 1175 (1991).
[24] *Landolt-Börnstein New Series, Group II*, edited by K. H. Hellwege and A. M. Hellwege (Springer-Verlag, Heidelberg, 1986), Vol. 16.
[25] A. Abragam and B. Bleaney, *Electron Paramagnetic Resonance of Transition Ions* (Dover, New York, 1986).
[26] N. W. Ashcroft and N. D. Mermin, *Solid State Physics* (Holt, Rinehart and Winston, New York, 1976).
[27] C. M. Varma, P. B. Littlewood, S. Schmitt-Rink, E. Abrahams, and A. E. Ruckenstein, Phys. Rev. Lett. **63**, 1996 (1989).
[28] D. C. Johnston and J. H. Cho, Phys. Rev. B **42**, 8710 (1990).
[29] T. C. Leung, X. W. Wang, and B. N. Harmon, Phys. Rev. B **37**, 384 (1988).
[30] B. Batlogg, in *High Temperature Superconductivity*, edited by K. S. Bedell, D. Coffey, D. E. Meltzer, D. Pines, and J. R. Schrieffer (Addison-Wesley, Redwood City, CA, 1990), pp. 37–82.
[31] C. Allgeier and J. S. Schilling, Phys. Rev. B **48**, 9747 (1993).
[32] M. v. Zimmermann, A. Vigliante, T. Niemöller, N. Ichikawa, T. Frello, S. Uchida, N. H. Andersen, J. Madsen, P. Wochner, J. M. Tranquada, D. Gibbs, and J. R. Schneider, Europhys. Lett. **41**, 629 (1998).
[33] N. B. Christensen, H. M. Rønnow, J. Mesot, R. A. Ewings, N. Momono, M. Oda, M. Ido, M. Enderle, D. F. McMorrow, and A. T. Boothroyd, Phys. Rev. Lett. **98**, 197003 (2007).
[34] E. Berg, E. Fradkin, E.-A. Kim, S. A. Kivelson, V. Oganesyan, J. M. Tranquada, and S. C. Zhang, Phys. Rev. Lett. **99**, 127003 (2007).
[35] M. Hücker, V. Kataev, J. Pommer, U. Ammerahl, A. Revcolevschi, J. M. Tranquada, and B. Büchner, Phys. Rev. B **70**, 214515 (2004).
[36] L. Li, J. G. Checkelsky, S. Komiya, Y. Ando, and N. P. Ong, Nat. Phys. **3**, 311 (2007).
[37] M. Oda, T. Nakano, K. Yamada, and M. Ido, Physica C **183**, 234 (1991).
[38] H.-H. Klauss, J. Phys.: Condens. Matter **16**, S4457 (2004).
[39] A. W. Hunt, P. M. Singer, A. F. Cederström, and T. Imai, Phys. Rev. B **64**, 134525 (2001).
[40] M. Hücker, Ph.D. thesis, University of Cologne, 1999.
[41] B. Vignolle, S. M. Hayden, D. F. McMorrow, H. M. Rønnow, B. Lake, C. D. Frost, and T. G. Perring, Nat. Phys. **3**, 163 (2007).
[42] R. Coldea, S. M. Hayden, G. Aeppli, T. G. Perring, C. D. Frost, T. E. Mason, S.-W. Cheong, and Z. Fisk, Phys. Rev. Lett. **86**, 5377 (2001).
[43] S.-W. Cheong, G. Aeppli, T. E. Mason, H. Mook, S. M. Hayden, P. C. Canfield, Z. Fisk, K. N. Clausen, and J. L. Martinez, Phys. Rev. Lett. **67**, 1791 (1991).
[44] K. Yamada, C. H. Lee, K. Kurahashi, J. Wada, S. Wakimoto, S. Ueki, H. Kimura, Y. Endoh, S. Hosoya, G. Shirane, R. J. Birgeneau, M. Greven, M. A. Kastner, and Y. J. Kim, Phys. Rev. B **57**, 6165 (1998).
[45] T. Imai, C. P. Slichter, K. Yoshimura, and K. Kosuge, Phys. Rev. Lett. **70**, 1002 (1993).
[46] S. Sugai, H. Suzuki, Y. Takayanagi, T. Hosokawa, and N. Hayamizu, Phys. Rev. B **68**, 184504 (2003).
[47] J. B. Torrance, A. Bezinge, A. I. Nazzal, T. C. Huang, S. S. P. Parkin, D. T. Keane, S. J. LaPlaca, P. M. Horn, and G. A. Held, Phys. Rev. B **40**, 8872 (1989).
[48] S. Wakimoto, K. Yamada, J. M. Tranquada, C. D. Frost, R. J. Birgeneau, and H. Zhang, Phys. Rev. Lett. **98**, 247003 (2007).
[49] O. J. Lipscombe, S. M. Hayden, B. Vignolle, D. F. McMorrow, and T. G. Perring, Phys. Rev. Lett. **99**, 067002 (2007).
[50] V. J. Emery and S. A. Kivelson, Phys. Rev. Lett. **74**, 3253 (1995).
[51] K. Takenaka, J. Nohara, R. Shiozaki, and S. Sugai, Phys. Rev. B **68**, 134501 (2003).
[52] C. C. Homes, S. V. Dordevic, G. D. Gu, Q. Li, T. Valla, and J. M. Tranquada, Phys. Rev. Lett. **96**, 257002 (2006).
[53] Y. S. Lee, K. Segawa, Z. Q. Li, W. J. Padilla, M. Dumm, S. V. Dordevic, C. C. Homes, Y. Ando, and D. N. Basov, Phys. Rev. B **72**, 054529 (2005).
[54] L. P. Gor'kov and G. B. Teitel'baum, Phys. Rev. Lett. **97**, 247003 (2006).
[55] Y. Ando, Y. Kurita, S. Komiya, S. Ono, and K. Segawa, Phys. Rev. Lett. **92**, 197001 (2004).
[56] H. Y. Hwang, B. Batlogg, H. Takagi, H. L. Kao, J. Kwo, R. J. Cava, J. J. Krajewski, and W. F. Peck, Jr., Phys. Rev. Lett. **72**, 2636 (1994).
[57] S. A. Kivelson, I. P. Bindloss, E. Fradkin, V. Oganesyan, J. M. Tranquada, A. Kapitulnik, and C. Howald, Rev. Mod. Phys. **75**, 1201 (2003).
[58] G. Y. Xu, J. M. Tranquada, T. G. Perring, G. D. Gu, M. Fujita, and K. Yamada, Phys. Rev. B **76**, 014508 (2007).
[59] G. Aeppli, T. E. Mason, S. M. Hayden, H. A. Mook, and J. Kulda, Science **278**, 1432 (1997).
[60] A. J. Millis and H. Monien, Phys. Rev. Lett. **70**, 2810 (1993).

[61] J. Schmalian, D. Pines, and B. Stojković, Phys. Rev. Lett. **80**, 3839 (1998).
[62] R. E. Walstedt, B. S. Shastry, and S.-W. Cheong, Phys. Rev. Lett. **72**, 3610 (1994).
[63] P. M. Singer, T. Imai, F. C. Chou, K. Hirota, M. Takaba, T. Kakeshita, H. Eisaki, and S. Uchida, Phys. Rev. B **72**, 014537 (2005).
[64] J. Haase, C. P. Slichter, R. Stern, C. T. Milling, and D. G. Hinks, Physica C **341-348**, 1727 (2000).
[65] P. Carretta, F. Tedoldi, A. Rigamonti, F. Galli, F. Borsa, J. H. Cho, and D. C. Johnston, Eur. Phys. J. B **10**, 233 (1999).
[66] G. B. Teitel'baum, B. Büchner, and H. de Gronckel, Phys. Rev. Lett. **84**, 2949 (2000).
[67] H.-J. Grafe, N. J. Curro, M. Hücker, and B. Büchner, Phys. Rev. Lett. **96**, 017002 (2006).
[68] H.-J. Grafe, N. J. Curro, B. L. Young, M. Hücker, J. Vavilova, A. Vyalikh, and B. Büchner (unpublished).